J. Fluid Mech. (1992), *vol.* 240, *pp.* 549–557
Printed in Great Britain

Gravity–capillary solitary waves in water of infinite depth and related free-surface flows

By JEAN-MARC VANDEN-BROECK[1] AND FRÉDÉRIC DIAS[2]

[1] Department of Mathematics and Center for the Mathematical Sciences, University of Wisconsin-Madison, Madison, WI 53705, USA

[2] INLN, Université de Nice, Parc Valrose, 06034 Nice, France

(Received 11 October 1991 and in revised form 10 December 1991)

Two-dimensional free-surface flows due to a pressure distribution moving at a constant velocity U at the surface of a fluid of infinite depth are considered. Both gravity g and surface tension T are included in the dynamic boundary condition. The velocity U is assumed to be smaller than $(4gT/\rho)^{\frac{1}{4}}$, so that there are no waves in the far field. Here ρ is the density of the fluid. The problem is solved numerically by a boundary integral equation technique. It is shown that for some values of U, four different flows are possible. Three of these flows are interpreted as perturbations of solitary waves in water of infinite depth. It is found that both elevation and depression solitary waves are possible in water of infinite depth. The numerical results for depression waves confirm and extend the solutions previously computed by Longuet-Higgins (1989).

1. Introduction

The two-dimensional free-surface flow due to a pressure distribution moving at a constant velocity U at the surface of a fluid of infinite depth is considered. The fluid is assumed to be inviscid and incompressible and the flow to be irrotational. The effects of gravity g and surface tension T are included in the free-surface boundary condition. A frame of reference moving with the pressure distribution is chosen, so that the flow is steady (see figure 1). At infinite depth the flow is characterized by a uniform stream with constant velocity U.

This problem was previously investigated by Rayleigh (1883) (see also Lamb 1932 p. 464 and Whitham 1974 p. 451).

Rayleigh assumed a distribution of pressure of small magnitude and linearized the equations around a uniform stream with constant velocity U. He solved the resulting linear equations in closed form. His results can be described in terms of the velocity

$$C_{\min} = \left(\frac{4gT}{\rho}\right)^{\frac{1}{4}} \tag{1.1}$$

Here ρ is density of the fluid.

For $U > C_{\min}$, Rayleigh's solutions are characterized by trains of waves in the far field. The wavenumber K of these waves satisfies the dispersion relation of linear gravity capillary waves:

$$U^2 = \frac{g}{K} + \frac{T}{\rho}K. \tag{1.2}$$

For $U > C_{\min}$, (1.2) has two distinct real roots $K = K_T$ and $K = K_g < K_T$. These two real roots merge as $U \to C_{\min}$. The waves corresponding to K_g and K_T appear behind the obstacle and ahead of the obstacle, respectively.

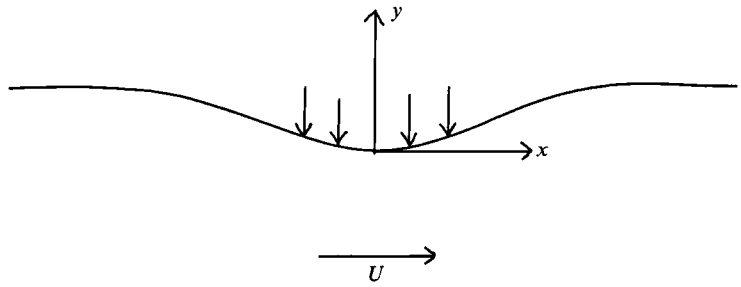

FIGURE 1. Sketch of the flow and of the coordinates.

For $U < C_{\min}$, Rayleigh's solutions do not predict waves in the far field and the flow approaches a uniform stream with constant velocity U at infinity. This is consistent with the fact that (1.2) does not have real roots for K when $U < C_{\min}$. The roots for K are complex when $U < C_{\min}$.

Rayleigh's solution is accurate for $U \neq C_{\min}$ in the limit as the magnitude of the pressure distribution approaches zero. However it is not uniform as $U \to C_{\min}$: for a given pressure distribution, the displacement of the free surface becomes unbounded as $U \to C_{\min}$. As we shall see, this non-uniformity is associated with branches of solitary waves bifurcating at $U = C_{\min}$. Such a bifurcation has been studied in finite depth by Iooss & Kirchgässner (1990).

In this paper we solve numerically the fully nonlinear free-surface flow due to a pressure distribution. We assume that $U < C_{\min}$, so that there are no waves in the far field. We show that for some values of U, four different flows are possible. For small pressure distributions, one of these flows is described by Rayleigh's solution. The other three flows are perturbations of solitary waves in water of infinite depth. Accurate computations of these solitary waves are presented. It is shown that there are both elevation and depression solitary waves. Our results for depression solitary waves confirm and extend the flows previously calculated by Longuet-Higgins (1989).

The problem is formulated in §2 and the numerical results are presented in §3.

2. Formulation

Let us consider the steady two-dimensional free-surface flow due to a pressure distribution acting on the surface of a fluid of infinite depth (see figure 1). At large depth the flow is characterized by a uniform stream with constant velocity U. We introduce Cartesian coordinates with the x-axis parallel to the velocity U at large depth and the y-axis directed vertically upwards. Gravity g is acting in the negative y-direction. The origin of the coordinates is chosen on the free surface and the pressure distribution is assumed to be symmetric with respect to $x = 0$.

We introduce the potential function $\phi(x, y)$ and the stream function $\psi(x, y)$. Without loss of generality, we choose $\psi = 0$ on the free surface and $\phi = 0$ at the point $x = 0$ on the free surface.

We introduce dimensionless variables by taking $T/\rho U^2$ as the unit length and U as the unit velocity. If u and v denote respectively the horizontal and the vertical components of the velocity, we write

$$f = \phi + \mathrm{i}\psi, \tag{2.1}$$

$$z = x + \mathrm{i}y, \tag{2.2}$$

$$u-\mathrm{i}v=\left(\frac{\mathrm{d}z}{\mathrm{d}f}\right)^{-1}=\frac{1}{x_\phi+\mathrm{i}y_\phi}. \tag{2.3}$$

We shall seek $x_\phi+\mathrm{i}y_\phi$ as an analytic function of f, in $\psi\leqslant 0$.

On the free surface the Bernoulli equation yields

$$\frac{1}{2}\frac{1}{x_\phi^2+y_\phi^2}+\alpha y+\frac{y_\phi x_{\phi\phi}-x_\phi y_{\phi\phi}}{(x_\phi^2+y_\phi^2)^{\frac{3}{2}}}+\epsilon P(\phi)=B, \tag{2.4}$$

where

$$\alpha=\frac{gT}{\rho U^4}. \tag{2.5}$$

Here $\epsilon P(\phi)$ is the prescribed distribution of pressure, B the Bernoulli constant and ρ the density of the fluid. We choose

$$P(\phi)=\begin{cases}\exp\left(\dfrac{1}{\phi^2-1}\right) & |\phi|\leqslant 1\\ 0 & \text{otherwise.}\end{cases} \tag{2.6}$$

Our assumption of $U<C_{\min}$ so that there are no waves in the far field means that $u-\mathrm{i}v\to 1$ as $|f|\to\infty$. It follows from (1.1) and (2.5) that $U=C_{\min}$ corresponds to $\alpha=\frac{1}{4}$. Therefore all our solutions will be characterized by $\alpha>\frac{1}{4}$.

We now apply the Cauchy integral formula to $x_\phi-1+\mathrm{i}y_\phi$ on a path consisting of the free surface $\psi=0$ and a semicircle at $\psi=-\infty$. Since $x_\phi-1+\mathrm{i}y_\phi\to 0$ as $\psi\to-\infty$, we have for $\psi<0$

$$x_\phi-1+\mathrm{i}y_\phi=-\frac{1}{2\pi\mathrm{i}}\int_{-\infty}^{+\infty}\frac{(x_\xi-1+\mathrm{i}y_\xi)|_{\psi=0}}{\xi-f}\,\mathrm{d}\xi,\quad \psi<0. \tag{2.7}$$

Setting $\psi=0$ in (2.7) and taking the real part we obtain

$$x_\phi=1-\frac{1}{\pi}\int_{-\infty}^{+\infty}\frac{y_\xi}{\xi-\phi}\,\mathrm{d}\xi,\quad \psi=0, \tag{2.8}$$

the integral being of Cauchy principal-value form.

Since the pressure distribution (2.6) is symmetric with respect to $\phi=0$, we use the symmetry of the flow to rewrite (2.8) as

$$x_\phi=1-\frac{1}{\pi}\int_0^\infty y_\xi\left[\frac{1}{\xi-\phi}+\frac{1}{\xi+\phi}\right]\mathrm{d}\xi. \tag{2.9}$$

Relations (2.4) and (2.9) define a nonlinear integro-differential equation for $x_\phi+\mathrm{i}y_\phi$ on the free surface.

We characterize the 'amplitude' of the free-surface displacement by the distance A between the origin of the coordinates and the level of the free surface at infinity. Thus

$$A=-y\quad\text{at}\quad|\phi|=\infty,\quad\psi=0. \tag{2.10}$$

The definition (2.10) implies that $A>0$ for elevation free-surface profiles and $A<0$ for depression free-surface profiles.

In order to solve the integro-differential equation ((2.4), (2.9)) numerically we introduce the mesh points

$$\phi_I=(I-1)E,\quad I=1,\ldots,N;$$
$$\phi_I^M=\tfrac{1}{2}E+(I-1)E,\quad I=1,\ldots,N-1;$$

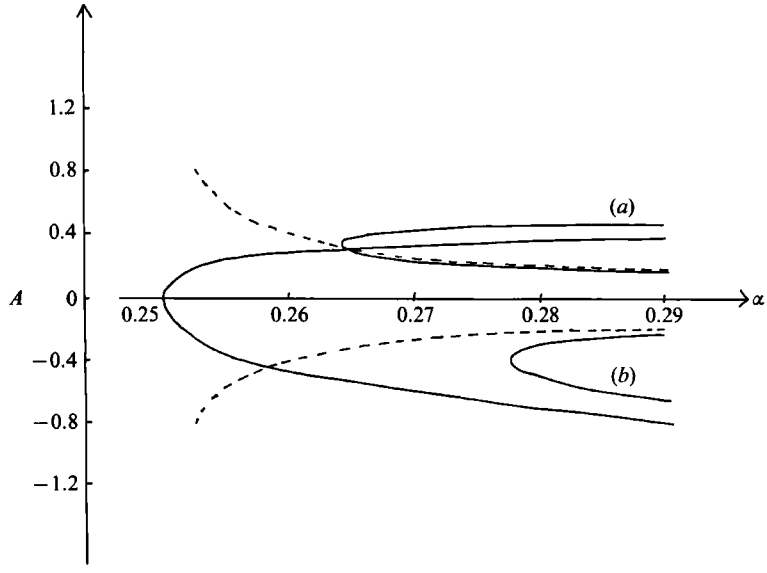

FIGURE 2. Values of A versus α. Curve (a) corresponds to $\epsilon = -0.1$; (b) corresponds to $\epsilon = 0.1$. The curves bifurcating from $\alpha = 0.25$ are the branches of solitary waves. The broken curves correspond to Rayleigh's solution for $\epsilon = \pm 0.1$.

and the unknowns

$$y'_I = y_\phi(\phi_I), \quad I = 1, \ldots, N.$$

Here E is the interval of discretization.

We evaluate (2.9) at the points ϕ_I^M. The integral is evaluated by the trapezoidal rule with a sum over the points ϕ_I. The symmetry of the quadrature and of the discretization, enables us to evaluate the Cauchy principal value as if it were an ordinary integral.

This gives $x_\phi(\phi_I^M)$ in terms of the unknowns y'_I. We evaluate

$$y_{\phi\phi}(\phi_I^M),\ x_{\phi\phi}(\phi_I^M),\ y_\phi(\phi_I^M)$$

in terms of y'_I by finite differences and interpolation. Next we express $y(\phi_I^M)$ in terms of y'_I by integrating y'_I by the trapezoidal rule. We then substitute all these expressions in (2.4) evaluated at ϕ_I^M, $I = 1, \ldots, N-2$. This leads to $N-2$ equations for the N unknowns y'_I, $I = 1, \ldots, N$. The last two equations are obtained by imposing the symmetry condition $y'_1 = 0$ and the truncation condition $y'_N = 0$. For fixed values of ϵ and α, this system of N nonlinear algebraic equations with N unknowns was solved by Newton's method. In order to handle the turning points in the (A, α)-plane (see next section) we also used a scheme in which ϵ and A are fixed and α is found as part of the solution.

Most of the computations were performed with $E = 0.11$ and $N = 400$. We checked that the results presented are independent of E and N to within graphical accuracy.

3. Discussion of the numerical results

The numerical scheme described in §2 was used to compute solutions for various values of α and ϵ. The properties of the solutions will be described by considering plots of A (see (2.10)) versus α (figures 2, 3 and 8). Typical free-surface profiles are shown in figures 4–7, 9 and 10.

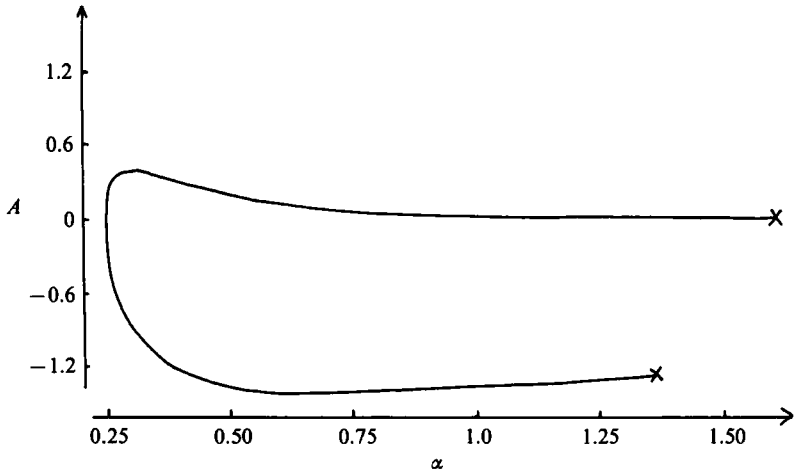

FIGURE 3. Values of A versus α for the branches of solitary waves. The crosses correspond to the limiting configurations with trapped bubbles shown in figures 6(*c*) and 7(*d*).

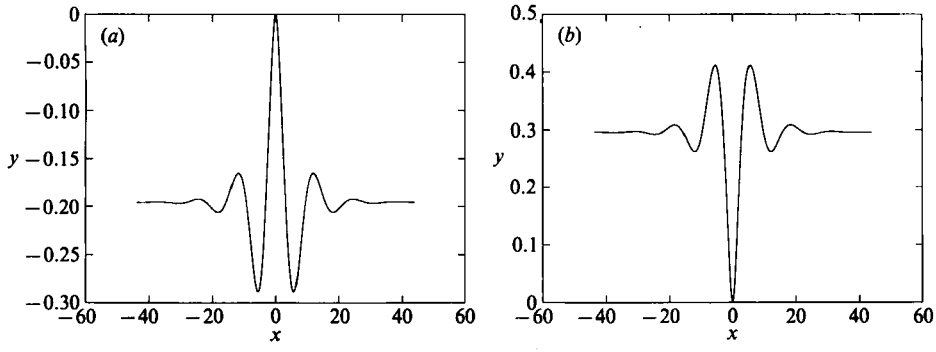

FIGURE 4. Free-surface profiles for $\alpha = 0.28$ and (*a*) $\epsilon = -0.1$, (*b*) $\epsilon = 0.1$. These profiles are closed to Rayleigh's solution.

Figure 2 shows two families of solutions corresponding to $\epsilon = -0.1$ (curve *a*) and $\epsilon = 0.1$ (curve *b*), with turning points at $\alpha \sim 0.264$ (curve *a*) and at $\alpha \sim 0.277$ (curve *b*). The broken curves in figure 2 are the results predicted by Rayleigh's solution for $\epsilon = \pm 0.1$. These curves show that Rayleigh's linear solution is not uniform as $\alpha \to 0.25$. For a fixed value of ϵ, $|A| \to \infty$ as $\alpha \to 0.25$. The solutions corresponding to the portions of curves (*a*) and (*b*) closest to the α-axis and extending from the turning points to $\alpha = \infty$ are close to the solutions calculated by Rayleigh for ϵ small. These solutions are perturbations of a uniform stream in the sense that they approach the uniform stream with constant velocity U as $|\epsilon| \to 0$. Typical free-surface profiles for $\alpha = 0.28$ are shown in figures 4(*a*) and 4(*b*).

The remaining portions of the curves (*a*) and (*b*) (i.e. the portions of the curves further away from the α-axis and extending to the right of the turning points) are not described by Rayleigh's calculations. Typical profiles for $\alpha = 0.28$ are shown in figures 5(*a*) and 5(*b*). As $|\epsilon| \to 0$, these solutions approach solitary wave configurations. The branches of solitary waves are shown in figures 2 and 3. Both elevation solitary waves (i.e. solutions with $A > 0$) and depression solitary waves (i.e. solutions with $A < 0$) are possible in water of infinite depth. These waves can be viewed as limits of

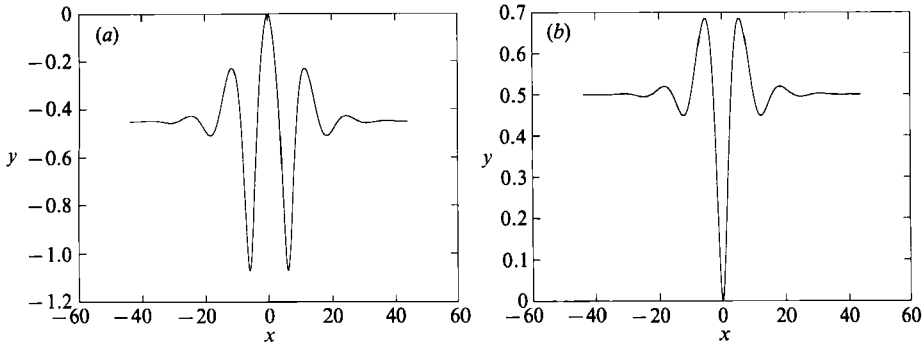

FIGURE 5. Free-surface profiles for $\alpha = 0.28$ and (*a*) $\epsilon = -0.1$, (*b*) $\epsilon = 0.1$. These profiles are perturbed solitary waves.

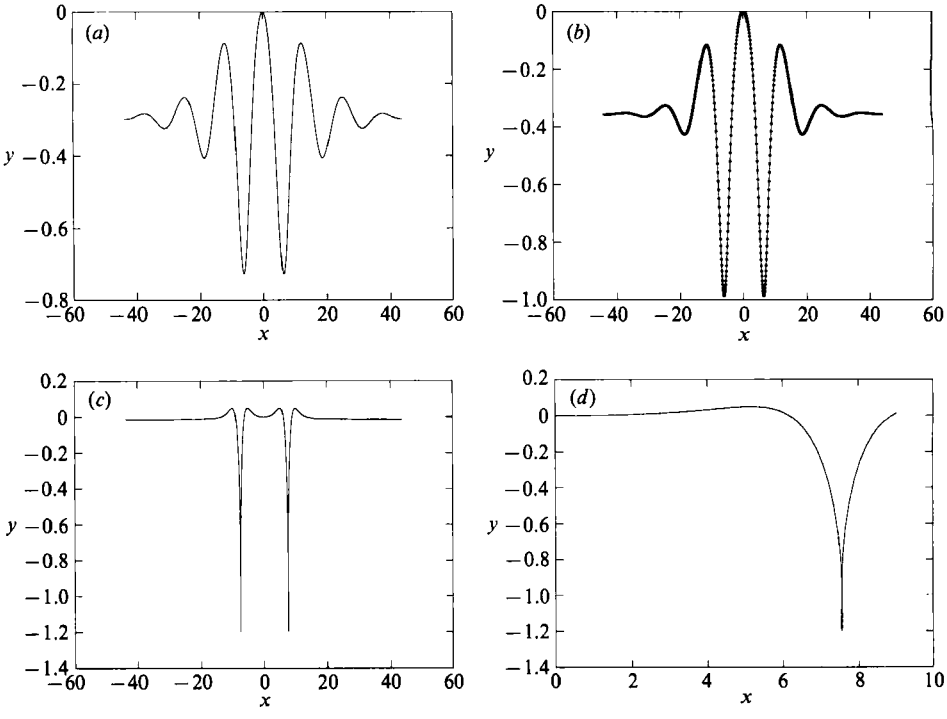

FIGURE 6. Free-surface profiles of elevation solitary waves for (*a*) $\alpha = 0.26$, (*b*) $\alpha = 0.275$, (*c*) $\alpha = 1.6$. The profile in (*c*) has two trapped bubbles at the troughs. A blow-up of one of these trapped bubbles is shown in (*d*). Plotted points are included in (*b*).

the solitary waves in water of finite depth of Iooss & Kirchgässner (1990) as the depth becomes infinite (see also Dias, Iooss & Vanden-Broeck 1992). Free-surface profiles of elevation and depression solitary waves in water of finite depth are shown in figures 6 and 7. Numerical values of A and of the maximum slope S of the free surface profiles are listed in table 1. Here S is calculated by finding the maximum of $\tan^{-1}(y_\phi/x_\phi)$ on the free surface.

The branches of solitary waves bifurcate from the uniform stream at $\alpha = 0.25$. Figures 6(*a*) and 7(*a*) show that the solitary waves approach a train of periodic waves as $\alpha \to 0.25$. The amplitude of this train of periodic waves approaches zero as $\alpha \to 0.25$.

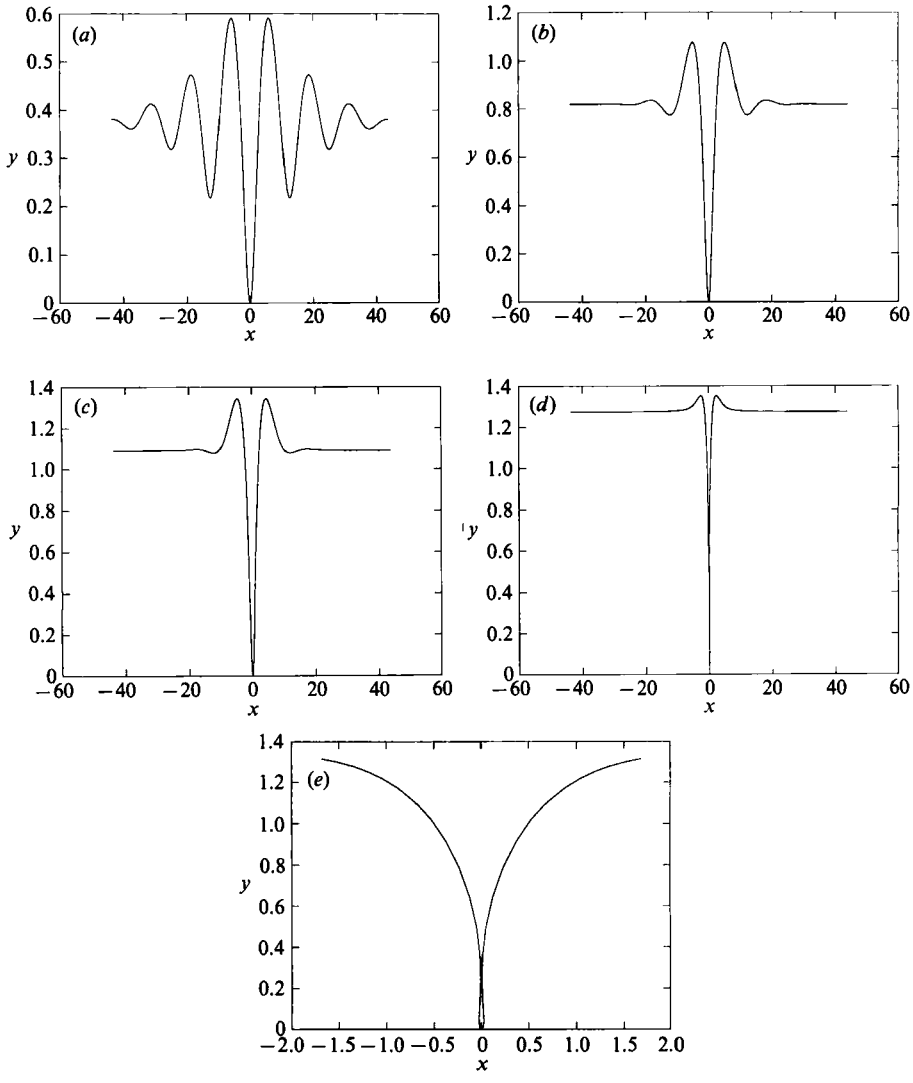

FIGURE 7. Free-surface profiles of depression solitary waves for (*a*) $\alpha = 0.255$, (*b*) $\alpha = 0.295$, (*c*) $\alpha = 0.350$, (*d*) $\alpha = 1.36$. The profile in (*d*) has a trapped bubble at its trough. A blow-up of this trapped bubble is shown in (*e*).

Elevation solitary waves			Depression solitary waves		
α	A	S	α	A	S
0.26	0.298	−0.20	0.255	−0.381	0.17
0.275	0.356	−0.30	0.295	−0.819	0.40
1.6	0.014	−1.57	0.350	−1.091	0.59
			1.36	−1.274	1.57

TABLE 1. Values of the parameters α, A and S for elevation and depression solitary waves

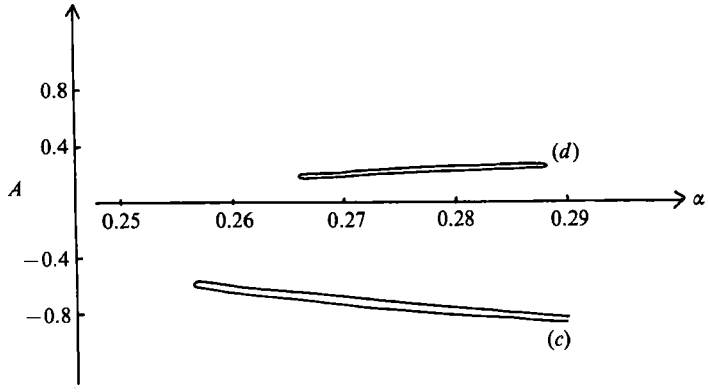

FIGURE 8. Values of A versus α. Curve (c) corresponds to a depression solitary wave perturbed by a negative ($\epsilon = -0.1$) pressure distribution; (d) corresponds to an elevation solitary wave perturbed by a positive ($\epsilon = 0.1$) pressure distribution.

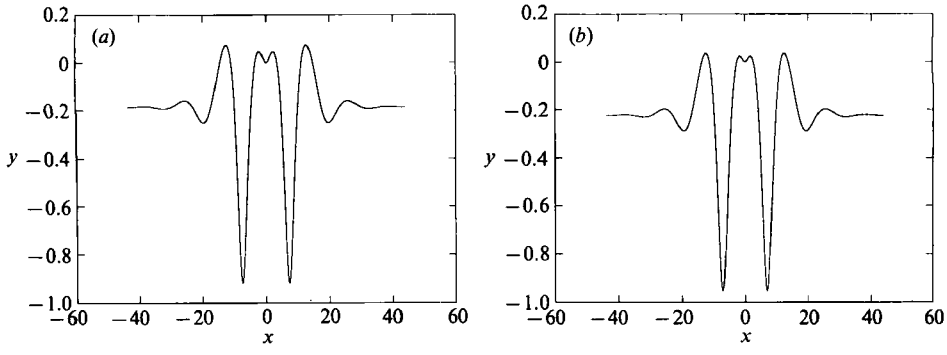

FIGURE 9. Free-surface profiles for $\alpha = 0.28$ and ($\epsilon = 0.1$). Both profiles are perturbations of elevation solitary waves.

As α increases, the solitary waves reach 'limiting' configurations with trapped bubbles. The elevation wave has two trapped bubbles (see figures 6c and 6d) and the depression wave has one trapped bubble (see figures 7d and 7e). Profiles for larger values of α could be obtained by following the analysis of Vanden-Broeck & Keller (1980).

Depression solitary waves in water of infinite depth were previously calculated by Longuet-Higgins (1989). Longuet-Higgins computed solutions in the range $0.35 \leqslant \alpha \leqslant 1.35$. We calculated the solutions shown in figure 3 of his paper and confirm his results. Figures 7(c) and 7(d) are in fact profiles corresponding to the solutions (f) and (a) in figure 3 of Longuet-Higgins' paper.

The portions of the curves (a) and (b) in figure 2 further away from the α-axis are elevation and depression solitary waves perturbed by negative ($\epsilon < 0$) and positive ($\epsilon > 0$) pressure distributions respectively. It was found that there are also solutions which are elevation solitary waves perturbed by a positive pressure distribution and solutions which are depression solitary waves perturbed by a negative pressure distribution. The corresponding curves in the (A, α)-plane for $\epsilon = \pm 0.1$ are shown in figure 8 (curves c and d). Typical profiles corresponding to $\alpha = 0.28$ are presented in figures 9 and 10. The curve for $\epsilon = 0.1$ in figure 8 is a closed curve (isola). The curve for $\epsilon = -0.1$ extends further to the right and only a portion of it is shown in figure 8.

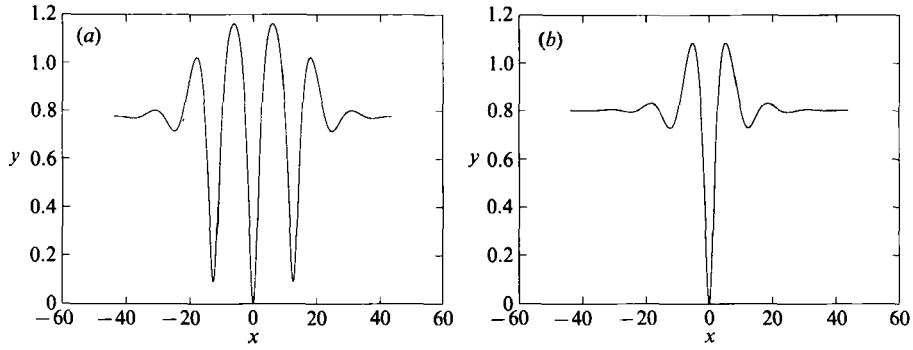

FIGURE 10. Free-surface profiles for $\alpha = 0.28$ and ($\epsilon = -0.1$). Both profiles are perturbations of depression solitary waves.

Finally, let us comment on the decaying oscillations present on the free-surface profiles as $|x| \to \infty$. These oscillations can be understood by considering the linear dispersion relation (1.2). In terms of the dimensionless variables, (1.2) becomes

$$K^2 - K + \alpha = 0. \tag{3.1}$$

For $\alpha > \frac{1}{4}$, (3.1) has the complex-conjugate roots $\frac{1}{2}[1 \pm \mathrm{i}(4\alpha - 1)^{\frac{1}{2}}]$. Therefore the free surfaces are characterized by oscillations of wavelength 4π and of amplitude decaying like $\exp[-(\alpha - \frac{1}{4})^{\frac{1}{2}}|x|]$ as $|x| \to \infty$. As α approaches $\frac{1}{4}$, these oscillations approach a slowly modulated train of waves. The existence of such a steady slowly modulated wave is consistent with the fact that the group velocity is equal to the phase velocity when $\alpha = \frac{1}{4}$. Analytical approximations for both elevation and depression solitary waves as $\alpha \to \frac{1}{4}$, will be reported in Dias *et al.* (1992).

REFERENCES

DIAS, F., IOOSS, G. & VANDEN-BROECK, J.-M. 1992 Capillary–gravity solitary waves with damped oscillations (in preparation).

IOOSS, G. & KIRCHGÄSSNER, K. 1990 *C.R. Acad. Sci. Paris* **311**, Ser. 1, 265.

LAMB, H. 1932 *Hydrodynamics*, 6th Edn. Cambridge University Press.

LONGUET-HIGGINS, M. 1989 *J. Fluid Mech.* **200**, 451.

RAYLEIGH, LORD 1883 *Proc. Lond. Math. Soc.* **15**, 69.

VANDEN-BROECK, J.-M. & KELLER, J. B. 1980 *J. Fluid Mech.* **98**, 161.

WHITHAM, G. B. 1974 *Linear and Nonlinear Waves*. Wiley.